

1 **Simultaneous activation of parallel sensory pathways promotes a grooming sequence in**
2 ***Drosophila*.**

3
4 Stefanie Hampel^{1,2}, Claire E. McKellar¹, and Julie H. Simpson^{1,3*}, Andrew M. Seeds^{1,2*}

5 ¹Janelia Research Campus, Howard Hughes Medical Institute, Ashburn, VA 20147

6 ²Current Address: Institute of Neurobiology, University of Puerto Rico-Medical Sciences

7 Campus, San Juan, Puerto Rico, 00901

8 ³Current address: Department of Molecular, Cellular, and Developmental Biology, University of

9 California, Santa Barbara, CA 93106, USA

10 *Correspondence

11

12 **Abstract**

13 A central model that describes how behavioral sequences are produced features a neural

14 architecture that readies different movements simultaneously, and a mechanism where

15 prioritized suppression between the movements determines their sequential performance. We

16 previously described a model whereby suppression drives a *Drosophila* grooming sequence that

17 is induced by simultaneous activation of different sensory pathways that each elicit a distinct

18 movement (Seeds et al. 2014). Here, we confirm this model using transgenic expression to

19 identify and optogenetically activate sensory neurons that elicit specific grooming movements.

20 Simultaneous activation of different sensory pathways elicits a grooming sequence that

21 resembles the naturally induced sequence. Moreover, the sequence proceeds after the sensory

22 excitation is terminated, indicating that a persistent trace of this excitation induces the next

23 grooming movement once the previous one is performed. This reveals a mechanism whereby

24 parallel sensory inputs can be integrated and stored to elicit a delayed and sequential grooming

25 response.

26

27 Introduction

28 A major question about nervous system function is how different movements are assembled to
29 form behavioral sequences. One of the primary models of sequential behavior is reminiscent of
30 how animals select among competing behavioral choices. Behavioral competition arises in
31 situations where different mutually exclusive behaviors are appropriate, but they must be
32 performed one at a time (Houghton and Hartley 1995; Redgrave, Prescott, and Gurney 1999).
33 These conflicts can be resolved through the suppression of all but the highest priority behavior,
34 as mollusks do to suppress their mating behavior while feeding (Davis 1979; Kupfermann and
35 Weiss 2001; Kristan 2008). In the case of a behavioral sequence, it is proposed that the
36 different movements to be performed are similarly readied in parallel and in competition for
37 output, and a suppression hierarchy determines their priority order of execution (Lashley 1951;
38 Houghton and Hartley 1995; Bullock 2004). Completion of the highest priority movement lifts
39 suppression on movements of lower priority that are subsequently performed according to a
40 new round of competition and suppression. This *parallel model* could drive behaviors across a
41 range of complexity, from the sequential typing of letters on a keyboard in humans to the
42 selection of which behavior to perform first in mollusks (Houghton and Hartley 1995). Thus, the
43 identification of examples of simple parallel neural architectures that drive a prioritized selection
44 of movements may inform a broad spectrum of sequential behaviors (Kristan 2014; Jovanic et
45 al. 2016).

46

47 A *Drosophila melanogaster* grooming sequence provides one example of how conflicting
48 stimuli can induce movement competition that is resolved through a suppression hierarchy.
49 Coating the body of a fly with dust is thought to stimulate competition among different grooming
50 movements that are each responsible for cleaning a particular body part (Phillis et al. 1993;
51 Seeds et al. 2014). We previously presented evidence that the body grooming order is
52 determined through a mechanism where earlier movements suppress later ones (Seeds et al.

53 2014). For example, removal of dust from the eyes occurs first because eye grooming
54 suppresses cleaning of the other body parts. From a suppression hierarchy among the different
55 grooming movements emerges a sequence that proceeds in the order: eyes > antennae >
56 abdomen > wings > notum. We further proposed a computational model to describe this
57 sequence that features parallel activation of the different grooming movements by dust to
58 induce competition, and hierarchical suppression among the movements to determine their
59 selection order (Seeds et al. 2014). The parallel activation of the movements was proposed
60 based on evidence that stimulation to each body part induces site-directed grooming responses
61 (Vandervorst and Ghysen 1980; Corfas and Dudai 1989; Seeds et al. 2014; Hampel et al.
62 2015). Thus, the simultaneous, or parallel stimulation of sensory neurons by dust would cause
63 different grooming movements to compete for output because only one can be performed at a
64 time. However, it was not confirmed that simultaneous activation of sensory neurons across the
65 body indeed elicits the same prioritized grooming response that we observed using a dust
66 stimulus.

67

68 Here, we reveal a neural basis for parallel activation of sensory inputs for a sequential
69 behavior by identifying sensory neurons that stimulate different grooming movements, and by
70 testing the hypothesis that activation of these neurons in parallel elicits a prioritized grooming
71 response. We identify transgenic expression tools for visualizing and optogenetically activating
72 sensory neurons on the body parts that elicit specific grooming movements. This enables the
73 simultaneous activation of sensory neurons across the body to induce competition among their
74 respective grooming movements. As we observed by coating the bodies of flies in dust, whole-
75 body sensory activation elicits grooming that prioritizes the head and then proceeds to the other
76 body parts. This provides direct evidence that the grooming sequence can be induced through
77 simultaneous activation of sensory neurons across the body. These experiments also reveal
78 that flies have a persistent trace of the body parts that were stimulated, which results in delayed

79 and sequential grooming of the stimulated parts. Work presented here lends neural-based
80 evidence to the parallel model of hierarchical suppression among grooming movements and
81 provides new insights into its underlying organization.

82

83 **Results**

84 ***GAL4 lines targeting sensory neurons across the body that elicit grooming***

85 Our initial goal was to identify GAL4 transgenic lines expressing in sensory neurons across the
86 body, to directly test whether simultaneous activation of these neurons leads to a prioritized
87 grooming response. As an entry point, we examined a collection of previously identified
88 enhancer-driven GAL4 lines that express in different neuronal populations whose activation
89 drove grooming (Seeds et al. 2014). Confocal microscopy imaging of the *peripheral nervous*
90 *system* (PNS) expression patterns of different lines from this collection revealed three that
91 express in sensory neurons across the body (R52A06-, R30B01-, and R81E10-GAL4; **Figure**
92 **1A-F**, R52A06-GAL4 shown as an example, **Figure 1 – figure supplement 1A-D**). We
93 classified the different sensory neuron types based on previous anatomical descriptions
94 (Murphey et al. 1989; Cole and Palka 1982; Dickinson and Palka 1987; Smith and Shepherd
95 1998; Kays, Cvetkovska, and Chen 2014) and found that the lines express predominantly in
96 mechanosensory neurons (**Figure 1G**). However, R30B01-GAL4 also showed expression in
97 chemosensory neurons (**Figure 1G**).

98

99 We next tested whether local populations of sensory neurons on specific body regions
100 can elicit individual grooming movements when focally activated. Site-directed grooming
101 responses have previously been investigated using tactile stimulation to particular
102 mechanosensory bristles on the body surface of decapitated flies (Vandervorst and Ghysen
103 1980; Corfas and Dudai 1989). Here, we used optogenetic activation with Channelrhodopsin,
104 directing blue light via an optical fiber to particular body regions of the broad sensory GAL4 lines

105 to activate sensory neurons on either the dorsal anterior or posterior body regions of
106 decapitated flies (**Figure 1 – figure supplement 2A,B**). Light directed to the posterior dorsal
107 body surface elicited grooming of the wings, whereas illumination of the anterior dorsal surface
108 elicited grooming of the notum (**Figure 1H, Video 1, Video 2**). This indicated that site-directed
109 grooming responses can be elicited optogenetically, and that the GAL4 lines express in sensory
110 neurons whose activation can elicit grooming movements for at least two parts of the body.

111

112 ***Simultaneous excitation of sensory neurons across the body induces a grooming***
113 ***sequence***

114 The GAL4 lines described above were next used to test a prediction of the model of hierarchical
115 suppression that simultaneous activation of sensory neurons across the body elicits head
116 grooming preferentially (Seeds et al. 2014). Freely moving flies of each line expressing the red
117 light-gated neural activator CsChrimson were exposed to whole body illumination to
118 optogenetically activate their targeted sensory neurons, and grooming responses were
119 subsequently measured. Each of the three GAL4 lines expresses in sensory neurons whose
120 activation can elicit wing or notum grooming, as revealed by localized optogenetic activation
121 (**Figure 1G,H**). Additionally, each line expresses in eye bristle mechanosensory neurons whose
122 activation we hypothesized could elicit eye grooming, while two of the lines (R52A06- and
123 R30B01-GAL4) also express in antennal Johnston's Organ neurons that were previously shown
124 to elicit antennal grooming (Hampel et al. 2015). Although these GAL4 lines can elicit several
125 movements from different body sensory neurons, we predicted that activating them
126 simultaneously should elicit only the highest-priority movement, according to the hierarchical
127 suppression model. Indeed, the simultaneous optogenetic activation of body sensory neurons
128 targeted by each GAL4 line resulted in head rather than posterior (abdomen, wing, notum)
129 grooming, consistent with the model of hierarchical suppression (**Figure 2A**, during red light-on
130 period).

131

132 Optogenetic activation of sensory neurons across the body also elicited a grooming
133 sequence reminiscent of dust-induced grooming. Flies groomed their heads at the onset of a
134 five-second red light stimulus, and then transitioned to grooming their posterior bodies during
135 the period after the light was turned off (**Figure 2A**). One trivial explanation for this sequence
136 could be that optogenetic activation of sensory neurons on the posterior body elicited grooming
137 with a latency, whereas there was no latency to groom with activation of the head sensory
138 neurons. We tested for this latency to groom the posterior body using decapitated flies that no
139 longer received a sensory drive to groom their heads. In contrast to intact flies, activation of the
140 posterior body sensory neurons of decapitated flies elicited posterior grooming during the red
141 light (**Figure 2B**). Thus, a latency does not explain the sequence because head and posterior
142 grooming can be elicited on similar time scales. Instead, evidence that intact flies do not display
143 posterior grooming with the light stimulation supports the hypothesis that it is suppressed by
144 head grooming (discussed below). Notably, optogenetic activation of sensory neurons across
145 the body causes flies to groom their bodies in the same order as when they were coated in dust
146 (head > abdomen > wings > notum) (**Figure 2 – figure supplement 2A,B, Video 3, Video 4,**
147 **and Video 5**). Further, the posterior body grooming sequence continued through the minute
148 after the cessation of the red light, while the sensory neurons were no longer activated (**Figure**
149 **2A, green histogram**). This suggests a persistent trace of posterior sensory neurons that had
150 been activated, which allowed each movement to be elicited once the previous grooming
151 movement terminated.

152

153 The behavior resulting from simultaneous activation of sensory neurons across the body
154 supports a role of suppression in establishing the grooming movement hierarchy. Evidence of
155 suppression was found when sensory neurons were reactivated during the period when flies
156 had transitioned to posterior grooming (**Figure 2A**). The hierarchical suppression model predicts

157 that switching the red light back on during this period to reactivate sensory neurons across the
158 body would result in head grooming, coupled with the termination of ongoing posterior
159 grooming. Indeed, in cases where flies were engaged in posterior grooming, delivery of the next
160 red light stimulus caused flies to terminate posterior grooming and switch to grooming their
161 heads. This is seen in **Figure 2A** (histogram plots on right, green traces) where the fraction of
162 flies grooming their posterior bodies drops to zero at the onset of the red light. Thus, we find
163 optogenetic-based evidence consistent with the hypothesis that the grooming sequence is driven
164 by a hierarchical suppression mechanism, as was revealed from experiments using natural
165 stimulus such as dust (Seeds et al. 2014).

166

167 ***Identification of mechanosensory neurons that elicit specific grooming movements***

168 We next sought to test whether the hierarchy of grooming movements could be observed with
169 competing activation of defined sets of sensory neurons that elicit distinct movements. We first
170 acquired transgenic lines for manipulating sensory neurons on specific body parts. Eye
171 grooming is the most hierarchically superior, and is thus elicited first in competition with other
172 grooming movements (Seeds et al. 2014). Based on previous work implicating the
173 interommatidial bristle mechanosensory neurons in eye grooming in the praying mantis and
174 cricket (Honegger 1977; Honegger, Reif, and Müller 1979; Zack and Bacon 1981), we found
175 that these neurons elicit eye grooming in *Drosophila*. A search through an image database of
176 brain expression patterns from the Vienna *Drosophila* collection identified a LexA line
177 (VT17251-LexA) that expressed exclusively in the interommatidial bristle mechanosensory
178 neurons. The hundreds of bristles on the compound eyes each contains the dendrite of a
179 sensory neuron, which also projects an axon into an afferent tract that enters the CNS in the
180 *subesophageal zone* (SEZ) (**Figure 3A,B**). In contrast to the praying mantis and cricket, the fly
181 eye bristle afferents project only to the SEZ, and not also the prothoracic neuromeres (**Figure**
182 **3B**). We tested whether activation of eye bristle mechanosensory neurons would elicit grooming

183 by expressing CsChrimson using VT17251-LexA and exposing flies to red light. Indeed,
184 optogenetic activation of the eye bristle mechanosensory neurons elicited eye grooming (**Figure**
185 **3C**).

186

187 We next acquired a transgenic driver line for manipulating sensory neurons that could
188 elicit wing grooming, which is lower in the hierarchy than eye grooming. From our previous
189 screen (Seeds et al. 2014), we identified a GAL4 line that expresses in neurons whose
190 activation could elicit wing grooming and showed expression in sensory neurons on the wings
191 (**Figure 4 – figure supplement 1A**, R31H10-GAL4, behavioral data not shown). However, the
192 identities of those sensory neurons were obscured by expression in other cells (**Figure 4 –**
193 **figure supplement 1B**). Therefore, we used the intersectional *Split GAL4* (spGAL4) technique
194 to restrict expression to only the sensory neurons (Luan et al. 2006; Pfeiffer et al. 2010).
195 spGAL4-mediated expression occurs only when the two GAL4 domains, the GAL4 *DNA binding*
196 *domain* (DBD) and the *transcriptional activation domain* (AD), are expressed in the same cells.
197 We generated spGAL4 flies that were anticipated to target the wing sensory neurons by
198 expressing the DBD in the pattern of R31H10-GAL4 and the AD in the pattern of R30B01-GAL4
199 (**Figure 4 – figure supplement 1B,C**).

200

201 The R30B01-AD \cap R31H10-DBD combination expresses in two main types of
202 mechanosensory neurons on the wings and halteres (**Figure 4A**). The first type includes
203 campaniform sensilla, which are dome-shaped structures on the fly cuticle that are each
204 innervated by a mechanosensory neuron that responds to deformations of the cuticle (Dickinson
205 and Palka 1987). Campaniform sensilla on the proximal part of the wing are largely clustered in
206 fields, whereas individual sensilla are found along the distal wing (Palka, Lawrence, and Hart
207 1979; Cole and Palka 1982; Palka et al. 1986; Dickinson and Palka 1987). R30B01-AD \cap
208 R31H10-DBD flies show a sparse labeling of neurons in the proximal fields (5 to 10 out of ~77

209 neurons (median = 6.5), **Figure 4A,B**, white asterisks), and expression in the majority of the
210 distal campaniform sensilla (5 to 6 out of 8 neurons (median = 5), **Figure 4A,C**, yellow
211 asterisks). The spGAL4 line also expresses in campaniform sensilla on the halteres (7 to 10 out
212 of ~139 neurons, **Figure 4E**). The other type of sensory neurons targeted by R30B01-AD \cap
213 R31H10-DBD are mechanosensory bristle neurons on the distal wing (expression in 3-5 out of
214 ~221 neurons (median = 3.5), **Figure 4A,D**, white arrowheads) (Hartenstein and Posakony
215 1989). These different neurons on the wings and halteres send projections to the *ventral*
216 *nervous system* (VNS), where they follow diverse paths locally, with some further ascending to
217 the SEZ in the brain (**Figure 4F**). The ascending afferents are likely from campaniform sensilla
218 on the halteres and proximal wings, whereas afferents that remain in the VNS are likely from
219 wing mechanosensory bristle neurons and distal campaniform sensilla (Palka, Lawrence, and
220 Hart 1979; Ghysen 1980; Dickinson and Palka 1987).

221

222 Optogenetic activation of the neurons targeted by R30B01-AD \cap R31H10-DBD
223 expressing CsChrimson elicited wing but not haltere grooming (**Figure 4G**). The parsimonious
224 explanation for this result is that the grooming was elicited by sensory neurons on the wing.
225 However, because the line also expresses in haltere campaniform sensilla, we cannot rule out
226 their involvement in the behavior. Nevertheless, the spGAL4 driver affords access to sensory
227 neurons for independent control of wing grooming.

228

229 ***Competition between eye and wing sensory neurons elicits prioritized grooming***

230 The hierarchical associations between eye and wing grooming were next examined by
231 activating their respective sensory pathways. We first compared the individual grooming
232 responses to acute activation of either the eye bristle mechanosensory neurons or the
233 wing/haltere sensory neurons. Flies were exposed to five-second pulses of red light, followed by

234 rest periods with no light. Activation of the eye bristle mechanosensory neurons elicited eye
235 grooming during the period when the red light was on that decayed when it turned off (**Figure**
236 **5A**, top, magenta). In contrast, activation of the wing/haltere sensory neurons elicited grooming
237 with the red light that persisted after light cessation (**Figure 5A**, middle, green). Importantly,
238 activation of either the eye bristle mechanosensory neurons or the wing sensory neurons alone
239 did not elicit the other corresponding grooming movement, or an anterior-to-posterior grooming
240 sequence. Thus, activation of these specific sensory types only elicits grooming of its
241 corresponding body part.

242

243 We next tested whether activation of the eye bristle mechanosensory neurons and
244 wing/haltere sensory neurons at the same time would elicit a prioritized eye grooming response,
245 as is predicted by the model. For this experiment, we identified a spGAL4 combination
246 (R31H10-AD \cap R34E03-DBD) that expressed both in the eye bristle mechanosensory neurons
247 and the same three categories of sensory neurons on the wings and halteres that were
248 expressed in the R30B01-AD \cap R31H10-DBD combination (**Figure 5B**). Simultaneous
249 optogenetic activation of these defined sensory neurons elicited prioritized grooming that started
250 with the eyes and then proceeded to the wings (**Figure 5A**, bottom), like what we observed with
251 activation of sensory neurons across the body (**Figure 2**). We also found evidence of
252 suppression by eye grooming, as ongoing grooming of the wings terminated and all flies
253 groomed their eyes with each red light stimulus (**Figure 5A**, bottom). These results demonstrate
254 the prioritization between grooming movements through direct optogenetic activation of the
255 sensory neurons that elicit grooming of specific body parts. This strengthens the conclusion of
256 our previous work that the sequence occurs when the grooming movements are activated in
257 parallel and then sequentially prioritized through hierarchical suppression (Seeds et al. 2014).

258

259 **Discussion**

260 The goal of this work was to test the prediction of the model of hierarchical suppression that
261 simultaneous activation of sensory neurons on different body parts elicits a prioritized grooming
262 response. Two lines of evidence led us to this prediction. The first was based on our previous
263 finding that coating the body of the fly in dust elicits grooming that prioritizes head over posterior
264 body grooming (Seeds et al. 2014). The second was based on data showing that local
265 stimulation to the body surface elicits site-specific grooming responses (Vandervorst and
266 Ghysen 1980; Corfas and Dudai 1989; Seeds et al. 2014; Hampel et al. 2015). Thus, we
267 proposed that sensory neurons across the body are stimulated in parallel by dust to elicit
268 competition among their respective grooming movements. Here, we test this by identifying
269 transgenic driver lines for targeting and directly activating sensory neurons that elicit grooming,
270 allowing us to bypass the dust stimulus and reveal the underlying sensory neurons. Using
271 simultaneous optogenetic activation of sensory neurons across the body we observe the same
272 anterior-to-posterior prioritization among the grooming movements that occurs when flies are
273 coated in dust. This lends strong support to the hypothesis that the grooming movements are
274 activated in parallel, and are thus selected in a hierarchically determined competition through
275 suppression.

276

277 ***Sensory neurons involved in grooming behavior***

278 One aim of this work was to identify sensory neurons that can induce grooming behavior. The
279 bristles are canonically thought to be involved in insect grooming based on evidence that their
280 tactile stimulation on different body parts induces site directed grooming responses
281 (Vandervorst and Ghysen 1980; Corfas and Dudai 1989; Page and Matheson 2004). Here, we
282 provide evidence that direct activation of the bristle mechanosensory neurons can elicit
283 grooming. We identify the fruit fly interommatidial bristle mechanosensory neurons based on
284 their anatomical similarity to those of the praying mantis and cricket (Honegger, Reif, and Müller
285 1979; Zack and Bacon 1981). Next, we use a transgenic driver line that expresses in these

286 neurons to show that their optogenetic activation elicits eye grooming. We also identified
287 different spGAL4 lines that express in neurons whose activation elicits wing grooming. However,
288 these lines express both in bristle mechanosensory neurons and campaniform sensilla, raising
289 the question of whether one or both sensory types are involved. Given the wealth of data
290 implicating the bristles in grooming (Tuthill and Wilson 2016), the parsimonious explanation is
291 that the wing bristle mechanosensory neurons are involved. However, there is also a precedent
292 for the involvement of non-bristle mechanosensory neurons such as the campaniform sensilla.
293 For example, we previously showed that Johnston's Organ chordotonal neurons can detect
294 displacements of the antennae to induce antennal grooming (Hampel et al. 2015), and others
295 have shown that gustatory neurons on the wing can detect different chemicals to trigger
296 grooming (Yanagawa, Guigue, and Marion-Poll 2014). Therefore, further work is required to
297 resolve which sensory neurons are involved in wing grooming.

298

299 One outstanding question is whether the sensory neurons have a direct role in
300 establishing hierarchical suppression. We previously proposed two mechanisms of hierarchical
301 suppression (Seeds et al. 2014). One is that unidirectional inhibitory connections between the
302 movements drive suppression, a mechanism not likely to involve the sensory neurons. The
303 other is that differences in sensitivity to dust across the body establish a gradient of sensory
304 drives among the grooming movements, leading to suppression through winner-take-all
305 competition. One way that sensitivity differences could be established is through differing
306 numbers of receptors on each body part. For example, if we assume that the bristle
307 mechanosensory neurons on the different body parts detect dust to elicit grooming (which
308 remains to be shown), a comparison of bristle numbers on different body parts gives mixed
309 support for this hypothesis. There are 600, 221, and 235 bristles reported to be on the eyes,
310 wings, and notum respectively (Hartenstein and Posakony 1989; Cadigan, Jou, and Nusse
311 2002). The eyes are the highest priority part to be groomed, and have 2.7 times more bristles

312 than the wings, which is consistent with the suppression hierarchy. In contrast, the lowest
313 priority body part is the notum, which has more bristles than the wings, arguing against the
314 hypothesis. Furthermore, given that other sensory neuron types elicit grooming (e.g.
315 chordotonal and gustatory neurons), there may be multiple ways of detecting dust (Yanagawa,
316 Guigue, and Marion-Poll 2014; Hampel et al. 2015). Alternatively, hierarchical suppression
317 could be established at the level of sensory neurons by regulating their output through
318 presynaptic inhibition (Blagburn and Sattelle 1987; Burrows and Matheson 1994; Clarac and
319 Cattaert 1996; Rudomin and Schmidt 1999). For example, the feeding behavior of the medicinal
320 leech causes presynaptic inhibition of mechanosensory neurons, which suppresses touch-
321 induced behavioral responses (Gaudry and Kristan 2009). Future experiments will test such
322 hypotheses about whether hierarchical suppression is established at the level of sensory
323 neurons.

324

325 ***Persistent neural activity within grooming neural circuits***

326 Emerging behavioral evidence indicates that neural circuits controlling *Drosophila* grooming
327 movements have mechanism(s) for maintaining excitability. This was originally proposed from a
328 study identifying a mechanosensory circuit that elicits persistent grooming of the antennae
329 (Hampel et al. 2015). That is, neurons within this circuit elicit grooming that continues for tens of
330 seconds beyond their optogenetic activation. Work presented here reveals that activation of
331 wing sensory neurons similarly elicits persistent grooming. Interestingly, grooming responses
332 that outlast their stimulus have also been described in vertebrates, suggesting that persistence
333 is a common feature of grooming (Sherrington 1906; Stein 2005). Despite the prevalence of
334 persistent grooming, its biological function remains unclear. One possibility is that persistence
335 prevents unnecessary switches between behaviors (Redgrave, Prescott, and Gurney 1999); for
336 example swimming responses can last beyond the initial stimulus so that an animal can safely

337 avoid a predator. In the case of grooming, persistence may ensure that a dirty body part is
338 thoroughly cleaned before switching to another behavior.

339

340 We also infer the maintenance of excitability within grooming neural circuits from the
341 observation that brief activation of sensory neurons across the body elicits a grooming
342 sequence. That is, flies groom their heads and then transition to their posterior bodies, even
343 during the period after the red light has turned off. This indicates that flies maintain a persistent
344 trace of which body parts are stimulated to elicit a delayed and sequential grooming response.
345 We postulate that this occurs when the simultaneous stimulation of sensory neurons across the
346 body activates each grooming movement in parallel. Eye grooming occurs first by suppressing
347 grooming movements occurring later (Seeds et al. 2014), however the circuitry for each later
348 movement remains active without requiring further sensory input. The next movement is then
349 elicited via this persistent neural activity once suppression from eye grooming ceases. If this is
350 the case, it raises the question of how the previous movement terminates to allow the next
351 movement to proceed. Further, it is unclear how circuits that drive later grooming movements
352 retain neural excitability. Such acquisition and maintenance of excitability is reminiscent of a
353 previously described feature of grooming called *temporal summation*, whereby successive
354 subthreshold stimuli are summed to elicit grooming (Sherrington 1906; Stein 2005; Guzulaitis,
355 Alaburda, and Hounsgaard 2013). Thus, both temporal summation and the grooming sequence
356 observed here point to a mechanism within the grooming neural circuitry that maintains a
357 persistent trace of the sensory stimulus.

358

359 How does a mechanism that maintains excitability within the grooming neural circuitry
360 affect our previously proposed model of grooming behavior? Our previous model indicated that
361 constant stimulation is necessary for each grooming movement to be active (Seeds et al. 2014).
362 That is, dust on a body part provides a constant drive to groom that is lessened through its

363 removal. Indeed, a computational model where the movements are driven entirely by the
364 presence of dust produces grooming that resembles dust-induced grooming. This indicates that
365 the model well describes grooming that occurs over relatively long time scales (~30 minutes).
366 However, based on observations that grooming persists after a brief stimulus, we now propose
367 that the circuitry contains a neural mechanism that allows grooming movements to remain
368 active on shorter time scales (tens of seconds). The ability to identify and manipulate the
369 sensory neurons that elicit grooming movements and their downstream circuits now enable
370 experiments to determine how persistent neural excitability is acquired and maintained.

371

372 **Methods**

373 ***Fly stocks and rearing conditions***

374 The GAL4 lines used in this study were produced by Gerald Rubin's lab at Janelia Research
375 Campus and are available from the Bloomington *Drosophila* stock center (Jenett et al. 2012).
376 The lines were identified in a screen for those that expressed GAL4 in neurons whose activation
377 could elicit grooming behavior (Seeds et al. 2014). In this work, we screened through the
378 images of the CNS expression patterns of these GAL4 lines (Jenett et al. 2012), searching for
379 those with expression in afferents from each of the different body parts (**Figure 1 – figure**
380 **supplement 1A-D**). These lines were selected for detailed behavioral and anatomical analysis
381 as described in the results section. The control used for the GAL4 lines was BDPGAL4U, which
382 contains the vector backbone used to generate each GAL4 line (including GAL4), but lacks any
383 enhancer to drive GAL4 expression (Seeds et al. 2014). The Split GAL4 stocks were produced
384 by Gerald Rubin's lab according to previously described methods (Pfeiffer et al. 2010).
385 VT17251-LexA was a gift from the lab of Barry Dickson. Controls for the Split GAL4 stocks were
386 produced in the same way as BDPGAL4U, but each spGAL4 half was used in place of GAL4
387 (Hempel et al. 2015).

388

389 Transgenic flies carrying the following UAS drivers were from the following citations:
390 *UAS-dTrpA1* (Hamada et al. 2008), *20xUAS-mCD8::GFP* (pJFRC7) (Pfeiffer et al. 2010),
391 *13xLexAop-myr::GFP* (pJFRC19) (Pfeiffer et al. 2010), *UAS-Channelrhodopsin-2* (Hwang et al.
392 2007), and *20xUAS-CsChrimson* (attP18) (Klapoetke et al. 2014). GAL4, spGAL4, and LexA
393 lines were crossed to their respective UAS or LexAop drivers, and the progeny were reared on
394 cornmeal and molasses food at 21°C and 50% relative humidity using a 16/8-hour light/dark
395 cycle. For optogenetic experiments using CsChrimson or ChR2, flies were reared in the dark on
396 food containing 0.4 mM all-*trans*-retinal. All experiments were done with five to eight day old
397 males.

398

399 ***Channelrhodopsin-mediated activation of sensory neurons using decapitated flies***

400 Two different regions of the bodies of decapitated flies were illuminated to locally activate
401 sensory neurons expressing ChR2. For decapitations, flies were cold-anesthetized, decapitated
402 using a standard razor blade, and allowed to recover for 10-20 minutes. The flies were
403 positioned on a slide for the experiment using a fine paint brush. A 473-nm blue light LED
404 (Nichia Corp, Tokushima, Japan) was attached to an optical fiber (1 mm in diameter) to direct
405 light to a specific region on the fly. The optical fiber was held approximately 1 mm from the
406 target body region to deliver a blue light stimulus with a luminance of 0.075 mW/mm². The light
407 was directed towards the dorsal posterior region, away from the anterior body, to activate
408 sensory neurons primarily on the wings (**Figure 1 – figure supplement 2A**). Alternatively, the
409 light was directed towards the dorsal anterior region, away from the posterior body, to activate
410 sensory neurons primarily on the notum (**Figure 1 – figure supplement 2B**). The LED stimulus
411 was controlled using a Grass SD9 stimulator (Astro-Med Inc., Warwick, RI) that delivered 10 Hz
412 pulses that were 20 milliseconds in duration, with 8-millisecond delays between pulses. Each fly
413 was subjected to stimulation on each body region in random order; however, in some cases the
414 flies would jump during the experiment and could not be used further. A grooming response to

415 the illuminated body region within a ten-second time frame was scored as a positive response.
416 The fraction of flies that responded was plotted. The number of trials for each dorsal body
417 region for each line were: R52A06-GAL4, anterior (n = 100), posterior (n = 100); R30B01-GAL4,
418 anterior (n = 40), posterior (n = 61); R81E10-GAL4, anterior (n = 86), posterior (n = 89).
419 Statistical significance was addressed using Chi-Square tests and Bonferroni correction.

420

421 ***CsChrimson-mediated activation of sensory neurons using freely moving flies***

422 The camera and behavioral setups used for recording freely moving flies with optogenetic
423 activation were described previously (Seeds et al. 2014; Hampel et al. 2015). Flies were cold
424 anesthetized, loaded into behavioral chambers, and allowed to recover for at least ten minutes.
425 R52A06-, R30B01-, and R81E10-GAL4 were used to express the light-gated channel
426 CsChrimson. The red light used for gating CsChrimson readily penetrates the fly cuticle (Inagaki
427 et al. 2014), allowing for uniform activation of sensory neurons across the body. Our initial
428 experiments using optogenetic activation of the neurons targeted by these GAL4 lines revealed
429 that high levels of red light activation caused defects in motor coordination. This was likely
430 caused by the strong activation of sensory neurons across the body, some of which are known
431 to be involved in proprioception (e.g. femoral chordotonal organs). Therefore, it was necessary
432 to reduce the red-light power to the point where it elicited grooming without causing coordination
433 defects. The light power that met these requirements for each GAL4 line are: R52A06-GAL4
434 (0.066 mW/mm²), R30B01-GAL4 (0.066 mW/mm²), and R81E10-GAL4 (0.077 mW/mm²). The
435 light power used for each LexA and spGAL4 line was: VT17251-LexA (0.382 mW/mm²),
436 R30B01-AD \cap R31H10-DBD and R31H10-AD \cap R34E03-DBD (0.135 mW/mm²). The red light
437 frequency was 5 Hz (0.1 seconds on/off) for 5 seconds, followed by 30 second intervals where
438 the red light was off. The experiment consisted of a total of three photostimulation periods with
439 30 second intervals between each stimulation. The experiment was recorded for manual
440 annotation of the grooming movements performed.

441

442 The recorded grooming movements of flies were manually annotated as described
443 previously (Seeds et al. 2014). For the ethogram and histogram plots in **Figure 2**, the different
444 head grooming movements (e.g. eye, antennal, and proboscis grooming) were binned (1
445 second time bins) and plotted as head grooming. Similarly, all movements that were directed
446 towards the body (e.g. abdomen, wings, notum) were binned and plotted as posterior body
447 grooming. Statistical analysis and display of the data were previously described (Hampel et al.
448 2015).

449

450 ***Analysis of CNS and PNS expression patterns***

451 Dissection and staining of the CNS was performed using a previously reported protocol (Hampel
452 et al. 2011). The head stain shown in **Figure 3A** was done as follows. Fine scissors were used
453 to cut off part of the proboscis and part of the eyes to improve antibody penetration. Heads were
454 fixed in phosphate buffered saline (PBS) containing 2% paraformaldehyde and 0.1% Triton for 2
455 hours at 4°C, and stained with primary antibodies: rabbit anti-GFP (1:500, Thermo Fisher
456 Scientific, Waltham, MA, #A11122) and mouse anti-nc82 (1:50, Developmental Studies
457 Hybridoma Bank, University of Iowa) followed by secondary antibodies: goat anti-rabbit DyLight
458 594 (Thermo Fisher Scientific #35560) and goat anti-mouse DyLight 633 (Thermo Fisher
459 Scientific #35512), with Calcofluor White to stain the cuticle (a few grains in 300 µl volume,
460 Sigma #F3543). Images were collected using a Zeiss LSM710 confocal microscope using a
461 Plan-Apochromat 20x/0.8 M27 objective (Carl Zeiss Corporation, Oberkochen, Germany).

462

463 Dissection of the different body parts and imaging of the PNS expression patterns of the
464 different GAL4, LexA, and Split GAL4 lines were performed as follows. The lines were crossed
465 to 20xUAS-*mCD8::GFP* (JFRC7) or 13xLexAop-*myr::GFP* (pJFRC19). The progeny were
466 anesthetized using CO₂, decapitated, dipped in 70% ethanol, transferred to PBS, and each

467 body part was dissected as described below. The unfixed body parts were imaged immediately
468 in PBS or Vectashield (Vector Laboratories, Burlingame, CA). We used both PBS and
469 Vectashield and did not notice a difference in the cell morphology or expression pattern when
470 using either reagent. The use of Vectashield had the advantage of resulting in fewer air bubbles
471 between the coverslip and sample.

472

473 *Head:* Flies were decapitated using a standard razor blade. Heads were then placed
474 “face up” on a slide in a small well that was made by stacking six reinforcement labels (Avery
475 Dennison Corporation, Brea, CA) and filled with PBS or Vectashield. A cover slip was then
476 placed over the well. *Abdomen:* The abdomen was severed from the rest of the body just
477 posterior to the scutellum. Abdomens were then placed on a slide in a well created as described
478 above. The abdomens were placed either ventral or dorsal side up so that each side could be
479 imaged. *Notum:* A scalpel was used to slice longitudinally between the legs and the dorsal side
480 of the notum. The notum was imaged in the same well preparation described above. *Wing:* A
481 scalpel was used to remove the left wing from the body of the fly. To ensure that the entire wing
482 was obtained, part of the body wall was also cut with the wing. The wing was then placed on a
483 drop of Vectashield and then covered with a coverslip. *Leg:* The left prothoracic leg was
484 dissected in the same way as the wing. All body parts were imaged using a Zeiss 710 confocal
485 microscope using 10x and 20x air objectives. Native GFP fluorescence was imaged using an
486 excitation wavelength of 488 nm, whereas autofluorescence from cuticle was imaged using 568
487 nm. Body parts from at least three flies were imaged from separate crosses on different days. In
488 some cases, the body parts were imaged at 20x and then stitched using a FIJI plugin (Preibisch,
489 Saalfeld, and Tomancak 2009).

490

491 The different sensory neuron types on each body part were classified based on previous
492 descriptions (Ghysen 1980; Cole and Palka 1982; Dickinson and Palka 1987; Murphey et al.

493 1989; Smith and Shepherd 1998). The numbers of campaniform sensilla and mechanosensory
494 bristle neurons on the wings were previously counted (Cole and Palka 1982; Dickinson and
495 Palka 1987; Hartenstein and Posakony 1989). Proximal campaniform sensilla described in this
496 work include ANWP, Teg, d.Rad.A, d.Rad.B, d.Rad.C, d.Rad.D, d.Rad.E, d.HCV, v.Rad.A,
497 v.Rad.B, v.Rad.C, v.HCV, and vL.III. Distal campaniform sensilla described in this work include
498 GSR, p.TSM, d.TSM, L3-V, ACV, L3-1, L3-2, and L3-3. We classified neurons on the wings as
499 bristle mechanosensory rather than chemosensory given that their dendrites appear to
500 terminate at the base of the bristle rather than projecting to the bristle tip.

501

502 **Acknowledgments**

503 We thank: David Shepherd for sharing his knowledge of sensory systems; Gerry Rubin and his
504 lab for generating the spGAL4 stocks used in this work; Aljoscha Nern for advice on identifying
505 eye bristle CNS expression patterns; Eric Hoopfer for Matlab code for producing histogram plots
506 and comments on the manuscript; Phuong Chung for help imaging body parts; Igor Siwanowicz
507 for suggestions on head staining methods; and Jonathan Blagburn for comments on the
508 manuscript. Funding for this work was provided by the Howard Hughes Medical Institute and the
509 COBRE Center for Neuroplasticity, NIH NIGMS P20GM103642.

510

511 **References**

512 Blagburn, Jonathan M, and David B Sattelle. 1987. "Presynaptic Depolarization Mediates
513 Presynaptic Inhibition at a Synapse Between an Identified Mechanosensory Neurone and Giant
514 Interneurone 3 in the First Instar Cockroach, *Periplaneta Americana*." *Journal of Experimental*
515 *Biology* 127 (1). The Company of Biologists Ltd: 135–57.
516
517 Bullock, Daniel. 2004. "Adaptive Neural Models of Queuing and Timing in Fluent Action." *Trends*
518 *in Cognitive Sciences* 8 (9): 426–33. doi:10.1016/j.tics.2004.07.003.

519

520 Burrows, M M, and T T Matheson. 1994. "A Presynaptic Gain Control Mechanism Among
521 Sensory Neurons of a Locust Leg Proprioceptor." *Journal of Neuroscience* 14 (1): 272–82.

522

523 Cadigan, Kenneth M, Austin D Jou, and Roel Nusse. 2002. "Wingless Blocks Bristle Formation
524 and Morphogenetic Furrow Progression in the Eye Through Repression of Daughterless."
525 *Development* 129 (14): 3393–3402.

526

527 Clarac, F, and D Cattaert. 1996. "Invertebrate Presynaptic Inhibition and Motor Control."
528 *Experimental Brain Research* 112 (2). doi:10.1007/BF00227635.

529

530 Cole, Eric S, and John Palka. 1982. "The Pattern of Campaniform Sensilla on the Wing and
531 Haltere of *Drosophila Melanogaster* And Several of Its Homeotic Mutants." *Journal of*
532 *Embryology and Experimental Morphology* 71 (October): 41–61.

533

534 Corfas, Gabriel, and Yadin Dudai. 1989. "Habituation and Dishabituation of a Cleaning Reflex in
535 Normal and Mutant *Drosophila*." *The Journal of Neuroscience* 9 (1): 56–62.

536

537 Davis, William J. 1979. "Behavioural Hierarchies." *Trends in Neurosciences* 2. Elsevier: 5–7.

538

539 Dickinson, M H, and J Palka. 1987. "Physiological Properties, Time of Development, and
540 Central Projection Are Correlated in the Wing Mechanoreceptors of *Drosophila*." *Journal of*
541 *Neuroscience* 7 (12): 4201–8.

542

543 Gaudry, Quentin, and William B Kristan. 2009. "Behavioral Choice by Presynaptic Inhibition of
544 Tactile Sensory Terminals." *Nature Neuroscience* 12 (11): 1450–57. doi:10.1038/nn.2400.

545

546 Ghysen, A. 1980. "The Projection of Sensory Neurons in the Central Nervous System of
547 *Drosophila*: Choice of the Appropriate Pathway." *Developmental Biology* 78 (2): 521–41.

548 doi:10.1016/0012-1606(80)90351-6.

549

550 Guzulaitis, Robertas, Aidas Alaburda, and Jørn Hounsgaard. 2013. "Increased Activity of Pre-
551 Motor Network Does Not Change the Excitability of Motoneurons During Protracted Scratch
552 Initiation." *Journal of Physiology* 591 (Pt 7): 1851–58. doi:10.1113/jphysiol.2012.246025.

553

554 Hamada, Fumika N, Mark Rosenzweig, Kyeongjin Kang, Stefan R Pulver, Alfredo Ghezzi,
555 Timothy J Jegla, and Paul A Garrity. 2008. "An Internal Thermal Sensor Controlling
556 Temperature Preference in *Drosophila*." *Nature* 454 (7201): 217–20. doi:10.1038/nature07001.

557

558 Hampel, Stefanie, Phuong Chung, Claire E McKellar, Donald Hall, Loren L Looger, and Julie H
559 Simpson. 2011. "*Drosophila* Brainbow: a Recombinase-Based Fluorescence Labeling
560 Technique to Subdivide Neural Expression Patterns." *Nature Methods* 8 (3): 253–59.

561 doi:10.1038/nmeth.1566.

562

563 Hampel, Stefanie, Romain Franconville, Julie H Simpson, and Andrew M Seeds. 2015. "A
564 Neural Command Circuit for Grooming Movement Control." *eLife* 4 (September).

565 doi:10.7554/eLife.08758.

566

567 Hartenstein, V, and J W Posakony. 1989. "Development of Adult Sensilla on the Wing and
568 Notum of *Drosophila Melanogaster*." *Development* 107 (2): 389–405.

569

570 Honegger, H W, H Reif, and W Müller. 1979. "Sensory Mechanisms of Eye Cleaning Behavior in

571 the Cricket *Gryllus Campestris*.” *Journal of Comparative Physiology a: Neuroethology, Sensory,*
572 *Neural, and Behavioral Physiology* 129 (3). Springer Berlin / Heidelberg: 247–56.
573
574 Honegger, Hans-Willi. 1977. “Interommatidial Hair Receptor Axons Extending Into the Ventral
575 Nerve Cord in the Cricket *Gryllus Campestris*.” *Cell and Tissue Research*.
576
577 Houghton, G, and T Hartley. 1995. “Parallel Models of Serial Behavior: Lashley Revisited.”
578 *Psyche* 2 (25): 1–25.
579
580 Hwang, Richard Y, Lixian Zhong, Yifan Xu, Trevor Johnson, Feng Zhang, Karl Deisseroth, and
581 W Daniel Tracey. 2007. “Nociceptive Neurons Protect *Drosophila* Larvae From Parasitoid
582 Wasps.” *Current Biology* 17 (24): 2105–16. doi:10.1016/j.cub.2007.11.029.
583
584 Inagaki, Hidehiko K, Yonil Jung, Eric D Hoopfer, Allan M Wong, Neeli Mishra, John Y Lin, Roger
585 Y Tsien, and David J Anderson. 2014. “Optogenetic Control of *Drosophila* Using a Red-Shifted
586 Channelrhodopsin Reveals Experience-Dependent Influences on Courtship.” *Nature Methods*
587 11 (3): 325–32. doi:10.1038/nmeth.2765.
588
589 Jenett, Arnim A, Gerald M Rubin, Teri-T B Ngo, David D Shepherd, Christine C Murphy,
590 Heather H Dionne, Barret D Pfeiffer, et al. 2012. “A GAL4-Driver Line Resource for *Drosophila*
591 Neurobiology.” *Cell Reports* 2 (4): 991–1001. doi:10.1016/j.celrep.2012.09.011.
592
593 Jovanic, Tihana, Casey Martin Schneider-Mizell, Mei Shao, Jean-Baptiste Masson, Gennady
594 Denisov, Richard Doty Fetter, Brett Daren Mensh, James William Truman, Albert Cardona, and
595 Marta Zlatic. 2016. “Competitive Disinhibition Mediates Behavioral Choice and Sequences in
596 *Drosophila*.” *Cell* 167 (3): 858–870.e19. doi:10.1016/j.cell.2016.09.009.

597

598 Kays, Ibrahim, Vedrana Cvetkovska, and Brian E Chen. 2014. "Structural and Functional
599 Analysis of Single Neurons to Correlate Synaptic Connectivity with Grooming Behavior." *Nature*
600 *Protocols* 9 (1): 1–10. doi:10.1038/nprot.2013.157.

601

602 Klapoetke, Nathan C, Yasunobu Murata, Sung Soo Kim, Stefan R Pulver, Amanda Birdsey-
603 Benson, Yong Ku Cho, Tania K Morimoto, et al. 2014. "Independent Optical Excitation of
604 Distinct Neural Populations." *Nature Methods* 11 (3): 338–46. doi:10.1038/nmeth.2836.

605

606 Kristan, William B. 2008. "Neuronal Decision-Making Circuits." *Current Biology* 18 (19): R928–
607 32. doi:10.1016/j.cub.2008.07.081.

608

609 Kristan, William B. 2014. "Behavioral Sequencing: Competitive Queuing in the Fly CNS."
610 *Current Biology* 24 (16): R743–46. doi:10.1016/j.cub.2014.06.071.

611

612 Kupfermann, Irving, and Klaudiusz R Weiss. 2001. "Motor Program Selection in Simple Model
613 Systems." *Current Opinion in Neurobiology* 11 (6): 673–77. doi:10.1016/S0959-4388(01)00267-
614 7.

615

616 Lashley, Karl Spencer. 1951. *Cerebral Mechanisms in Behavior*. Edited by Lloyd A Jeffress.
617 New York: Wiley.

618

619 Luan, Haojiang, Nathan C Peabody, Charles R Vinson, and Benjamin H White. 2006. "Refined
620 Spatial Manipulation of Neuronal Function by Combinatorial Restriction of Transgene
621 Expression." *Neuron* 52 (3): 425–36. doi:10.1016/j.neuron.2006.08.028.

622

- 623 Murphey, R K, D R Possidente, P Vandervorst, and A Ghysen. 1989. "Compartments and the
624 Topography of Leg Afferent Projections in *Drosophila*." *Journal of Neuroscience* 9 (9): 3209–17.
625
- 626 Page, Keri L KL, and Thomas T Matheson. 2004. "Wing Hair Sensilla Underlying Aimed Hindleg
627 Scratching of the Locust." *Journal of Experimental Biology* 207 (Pt 15): 2691–2703.
628 doi:10.1242/jeb.01096.
629
- 630 Palka, J, M A Malone, R L Ellison, and D J Wigston. 1986. "Central Projections of Identified
631 *Drosophila* Sensory Neurons in Relation to Their Time of Development." *Journal of*
632 *Neuroscience* 6 (6): 1822–30.
633
- 634 Palka, John, Peter A Lawrence, and H Stephen Hart. 1979. "Neural Projection Patterns From
635 Homeotic Tissue of *Drosophila* Studied in Bithorax Mutants and Mosaics." *Developmental*
636 *Biology* 69 (2): 549–75. doi:10.1016/0012-1606(79)90311-7.
637
- 638 Pfeiffer, B D, T-T B Ngo, K L Hibbard, C Murphy, A Jenett, J W Truman, and G M Rubin. 2010.
639 "Refinement of Tools for Targeted Gene Expression in *Drosophila*." *Genetics* 186 (2): 735–55.
640 doi:10.1534/genetics.110.119917.
641
- 642 Phillis, R W, A T Bramlage, C Wotus, A Whittaker, L S Gramates, D Seppala, F Farahanchi, P
643 Caruccio, and R K Murphey. 1993. "Isolation of Mutations Affecting Neural Circuitry Required for
644 Grooming Behavior in *Drosophila Melanogaster*." *Genetics* 133 (3). Genetics Soc America:
645 581–92.
646
- 647 Preibisch, Stephan, Stephan Saalfeld, and Pavel Tomancak. 2009. "Globally Optimal Stitching
648 of Tiled 3D Microscopic Image Acquisitions." *Bioinformatics* 25 (11): 1463–65.

649 doi:10.1093/bioinformatics/btp184.

650

651 Redgrave, P, T J Prescott, and K Gurney. 1999. "The Basal Ganglia: a Vertebrate Solution to
652 the Selection Problem?." *Neuroscience* 89 (4): 1009–23. doi:10.1016/S0306-4522(98)00319-4.

653

654 Rudomin, P, and Robert F Schmidt. 1999. "Presynaptic Inhibition in the Vertebrate Spinal Cord
655 Revisited." *Experimental Brain Research* 129 (1): 1–37. doi:10.1007/s002210050933.

656

657 Seeds, Andrew M, Primoz Ravbar, Phuong Chung, Stefanie Hampel, Frank M Midgley, Brett D
658 Mensh, and Julie H Simpson. 2014. "A Suppression Hierarchy Among Competing Motor
659 Programs Drives Sequential Grooming in *Drosophila*." *eLife* 3: e02951.

660

661 Sherrington, Charles S. 1906. *The Integrative Action of the Nervous System*. New York: Charles
662 Scribner's sons.

663

664 Smith, S A, and D Shepherd. 1998. "Central Afferent Projections of Proprioceptive Sensory
665 Neurons in *Drosophila* Revealed with the Enhancer-Trap Technique." *The Journal of*
666 *Comparative Neurology* 364 (2). Wiley Online Library: 311–23.

667

668 Stein, PSG. 2005. "Neuronal Control of Turtle Hindlimb Motor Rhythms." *Journal of*
669 *Comparative Physiology A*.

670

671 Tuthill, John C, and Rachel I Wilson. 2016. "Mechanosensation and Adaptive Motor Control in
672 Insects." *Current Biology : CB* 26 (20): R1022–38. doi:10.1016/j.cub.2016.06.070.

673

674 Vandervorst, Philippe, and Alain Ghysen. 1980. "Genetic Control of Sensory Connections in

675 *Drosophila.*” *Nature* 286 (5768): 65–67. doi:10.1038/286065a0.

676

677 Yanagawa, Aya, Alexandra M A Guigue, and Frédéric Marion-Poll. 2014. “Hygienic Grooming Is

678 Induced by Contact Chemicals in *Drosophila Melanogaster.*” *Frontiers in Behavioral*

679 *Neuroscience* 8: 254–54. doi:10.3389/fnbeh.2014.00254.

680

681 Zack, S S, and J J Bacon. 1981. “Interommatidial Sensilla of the Praying Mantis: Their Central

682 Neural Projections and Role in Head-Cleaning Behavior.” *Journal of Neurobiology* 12 (1): 55–

683 65. doi:10.1002/neu.480120105.

684

685

686

687

688

689

690

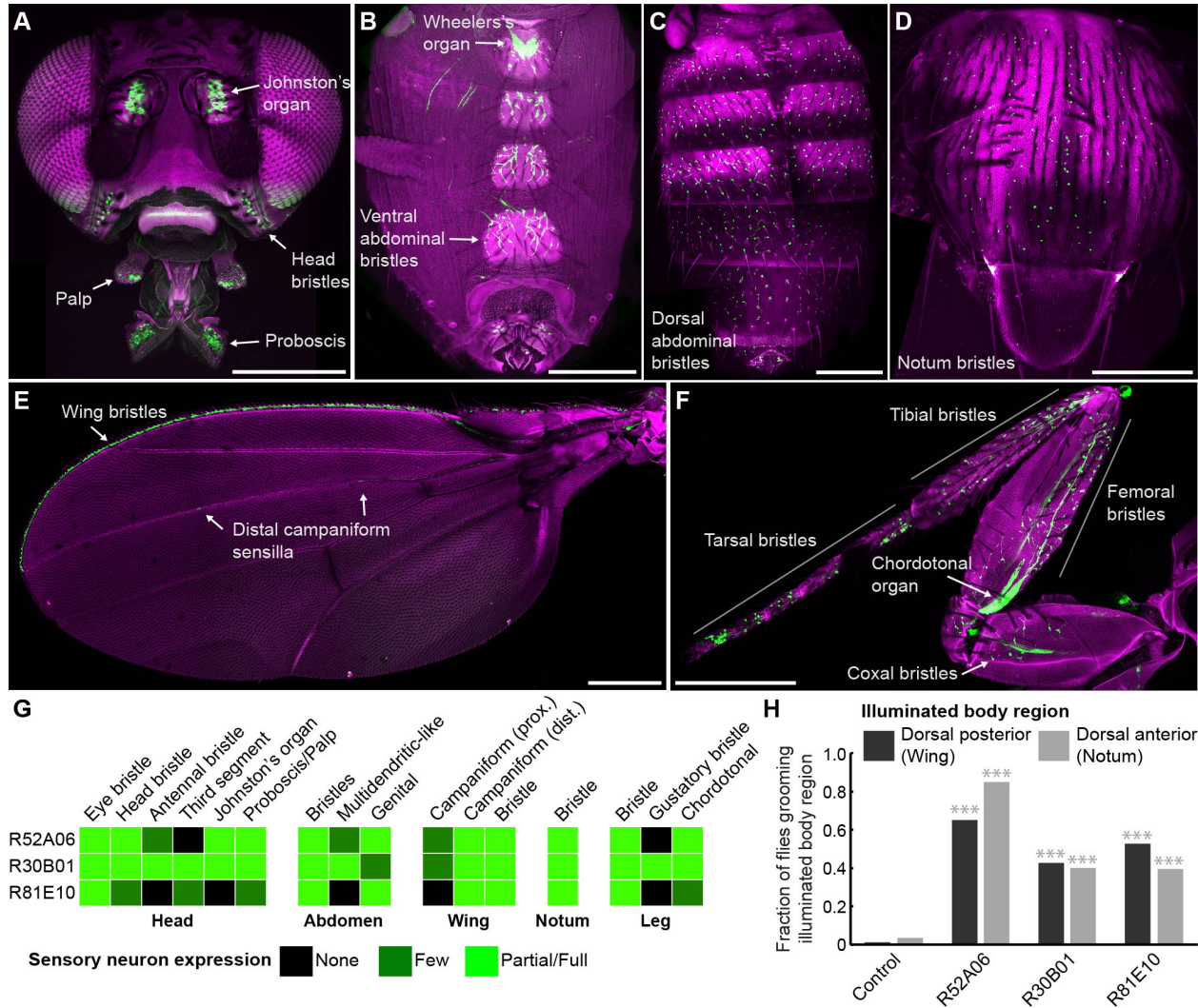
691

692

693

694

695



696

697 **Figure 1. GAL4 lines expressing in sensory neurons whose activation elicits grooming.**

698 (A-E) Peripheral expression pattern of R52A06-GAL4 expressing *green fluorescent protein*

699 (GFP). Confocal maximum projections are shown. Sensory neurons are in green and

700 autofluorescence from the cuticle is in magenta. Body parts shown are: (A) head, (B) ventral

701 abdomen, (C) dorsal abdomen, (D) notum, (E) wing, and (F) prothoracic leg. Labeled arrows

702 indicate specific sensory classes. In (C) and (D) all GFP positive cells are bristle

703 mechanosensory neurons. Scale bars, 250 μ m. (G) Summary table of the expression patterns

704 of R52A06-, R30B01-, and R81E10-GAL4 in sensory neurons on each indicated body part. (H)

705 Grooming responses to optogenetic activation of sensory neurons targeted by different GAL4

706 lines expressing ChR2. An optical fiber connected to an LED was used to direct light to the
707 dorsal surface of the anterior or posterior body (**Figure 1 – figure supplement 2**). The fraction
708 of flies that showed a grooming response to the blue light-illuminated body region is plotted ($n \geq$
709 40 trials for each body part). Grey shades and labels indicate the region that was illuminated.
710 Chi-squared test, Asterisks: $p < 0.0001$. See **Video 1** and **Video 2** for representative examples.

711

712

713

714

715

716

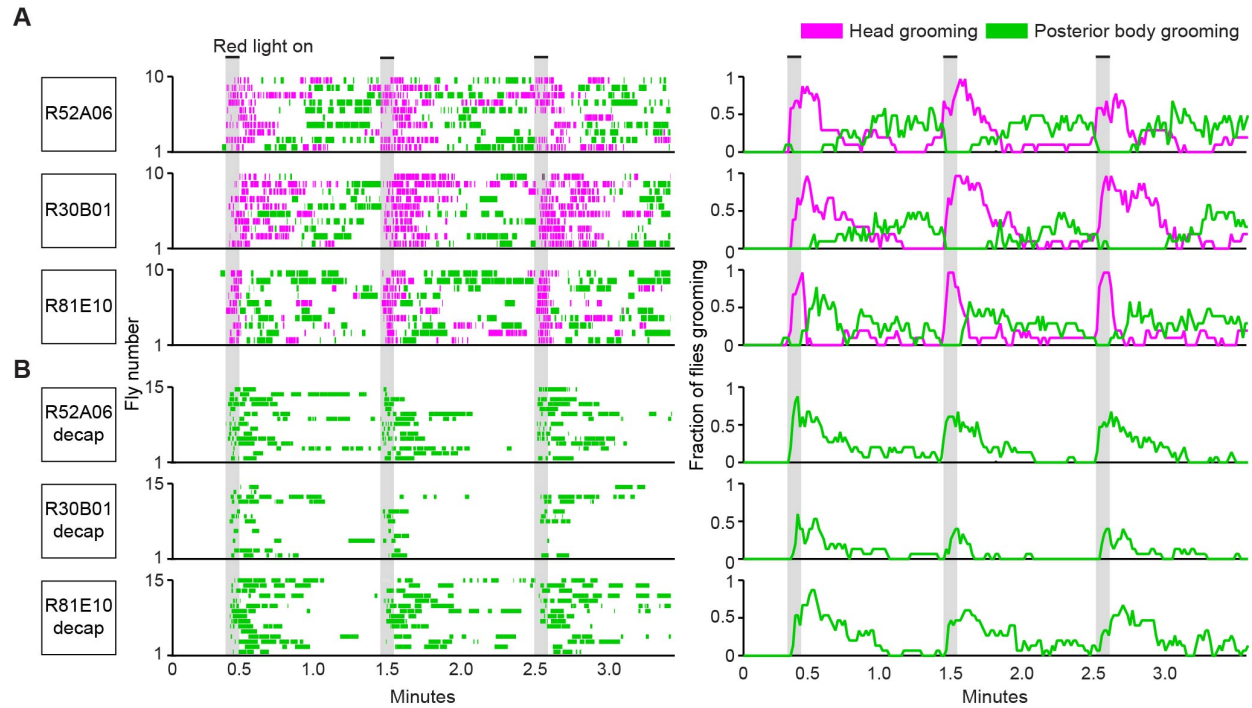
717

718

719

720

721



722

723 **Figure 2. Simultaneous optogenetic activation of body sensory neurons elicits sequential**

724 **grooming. (A-B)** Head (magenta) or posterior body grooming movements (green) elicited with

725 red light-illumination of R52A06-, R30B01-, and R81E10-GAL4 flies expressing CsChrimson.

726 The movements are mutually exclusive. Ethograms of ten individual flies are stacked for each

727 line (left). Histograms show the fraction of flies that were performing specific grooming

728 movements within one-second time bins (right). Gray bars indicate five second presentations of

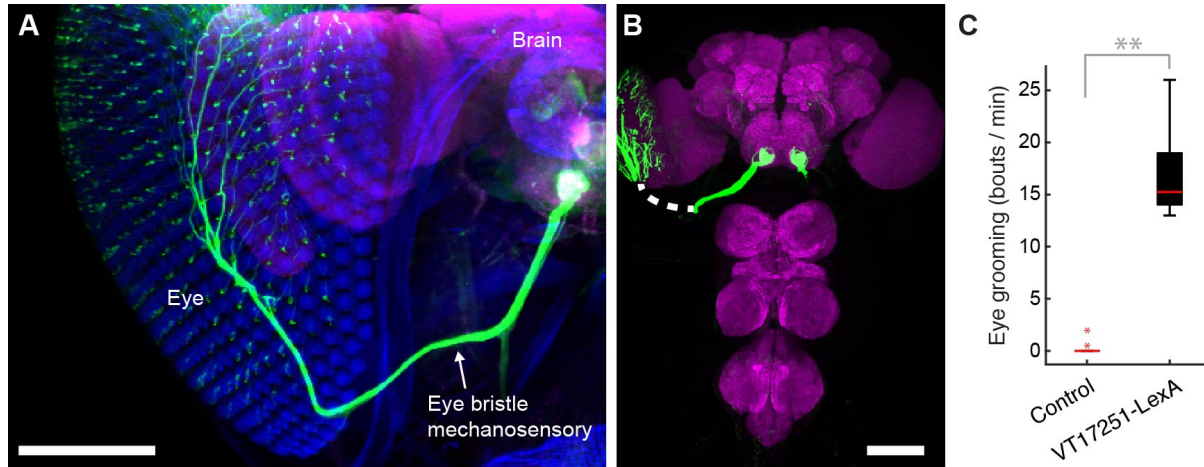
729 red light. **(A)** Grooming movements performed by intact flies. **(B)** Grooming movements

730 performed by decapitated flies. See **Video 3**, **Video 4**, and **Video 5** for representative

731 examples. Red light illumination of control flies did not elicit grooming (**Figure 2 – figure**

732 **supplement 1**).

733



734

735 **Figure 3. Interommatidial bristle mechanosensory neurons elicit eye grooming. (A-B)** The

736 expression pattern of VT17251-LexA in eye bristle mechanosensory neurons. The neurons

737 were stained with anti-GFP (green) and the brain neuropile is stained with anti-Bruchpilot

738 (magenta). Both images are maximum intensity projections. Scale bars, 100 μ m. (A) Expression

739 pattern shown in the semi-intact head. The eye and head cuticle is shown in blue. (B)

740 Expression pattern in the CNS. White dashed line indicates the trajectory of eye bristle

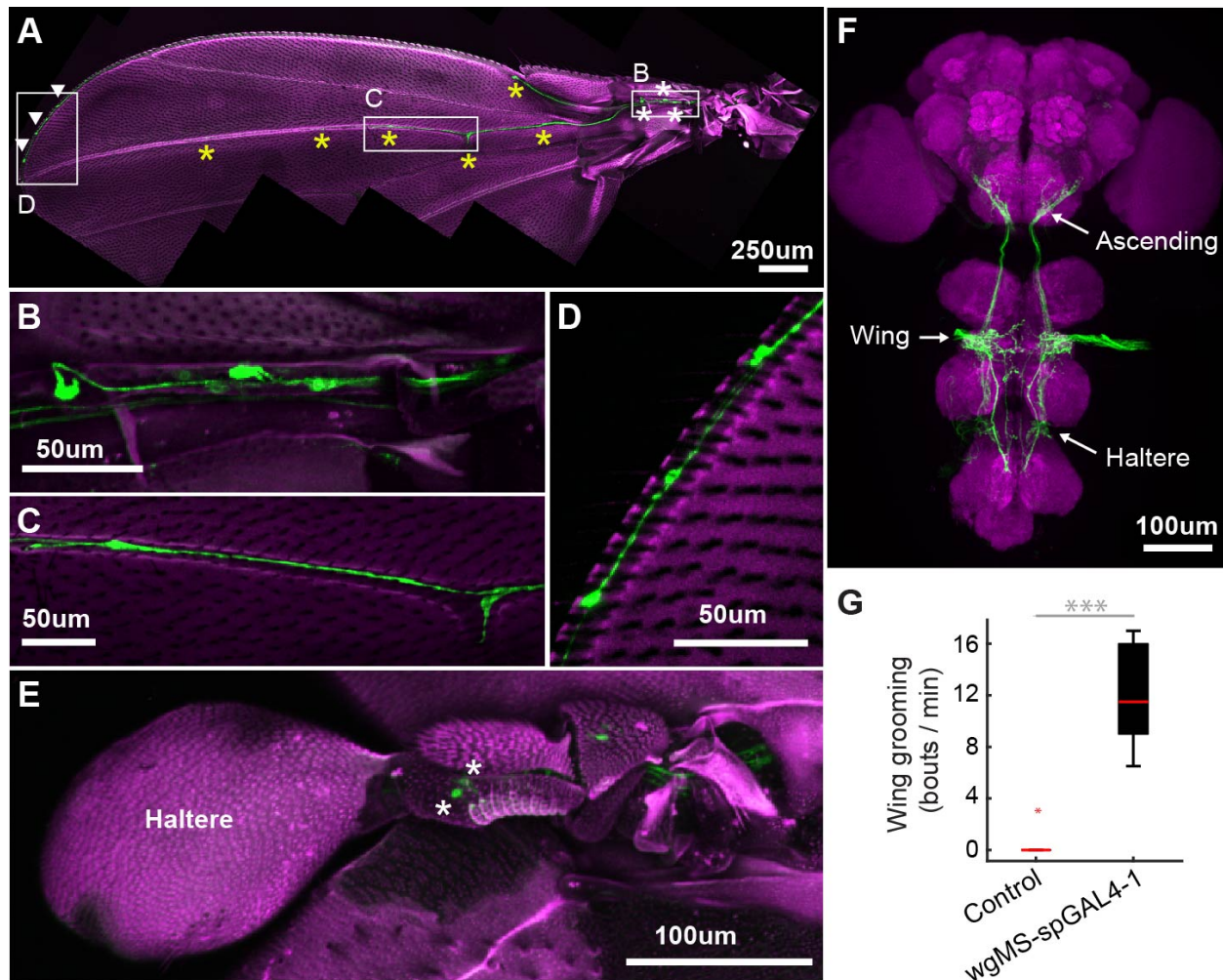
741 mechanosensory neuron axons found from the more intact preparations in (A). (C) Eye

742 grooming bout rate with optogenetic activation of neurons targeted by VT17251-LexA. Bottom

743 and top of the boxes indicate the first and third quartiles respectively; median is the red line;

744 whiskers show the upper and lower 1.5 IQR; red dots are data outliers (n = 10 for each box;

745 asterisks show $p < 0.001$, Kruskal-Wallis and post hoc Mann-Whitney U pairwise test).



746

747

748

749

750

751

752

753

754

755

756

Figure 4. spGAL4 driver that expresses in wing and haltere sensory neurons whose activation elicits wing grooming. (A-E) The expression pattern of R30B01-AD \cap R31H10-DBD in sensory neurons of the wings and halteres. Native GFP fluorescence is shown in green and autofluorescence from the cuticle is in magenta. Maximum intensity projections are shown. The proximal wing is to the right and the distal wing is to the left. (A) Sensory neurons on the wing. White boxes and letters indicate the regions shown in B-D. The different symbols indicate the sensory neuron types on the wing as proximal campaniform sensilla (white asterisks), distal campaniform sensilla (yellow asterisks), or bristle mechanosensory (white arrowheads). Scale bar, 250 μ m. (B-D) Larger images of the regions shown in A. Scale bars, 50 μ m. Shown are the proximal campaniform sensilla (B), distal campaniform sensilla (C), and bristle mechanosensory

757 neurons (**D**). (**E**) Expression in the haltere campaniform sensilla (asterisks). Scale bar, 100 μ m
758 (**F**) CNS expression visualized by co-stain with anti-GFP (green) and anti-Bruchpilot (magenta).
759 Arrows indicate the CNS entry points of afferents from the wings and halteres, and the location
760 of ascending projections from some of these afferents. Scale bar, 100 μ m. (**C**) Wing grooming
761 bout rate with optogenetic activation of neurons targeted by R30B01-AD \cap R31H10-DBD. Data
762 are displayed as described for **Figure 3C**. Asterisks: $p < 0.0001$.

763

764

765

766

767

768

769

770

771

772

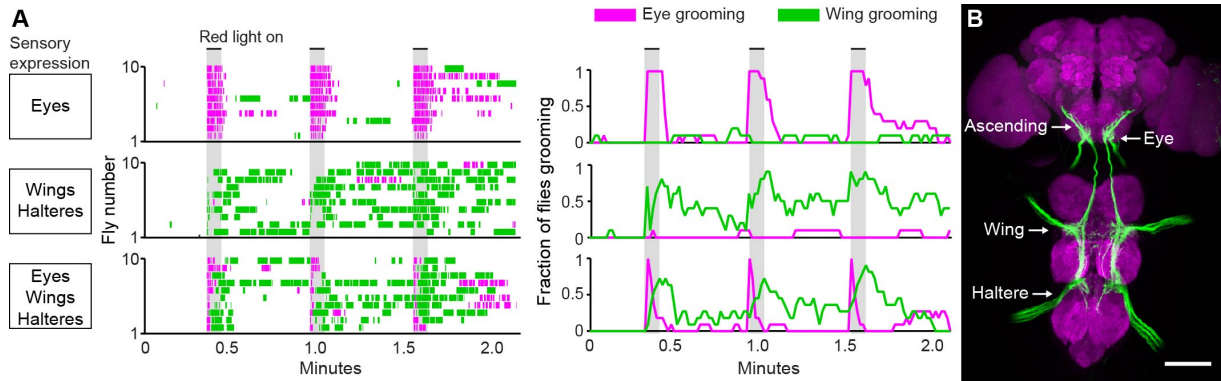
773

774

775

776

777



778

779 **Figure 5. Simultaneous excitation of eye and wing/haltere sensory neurons produces**

780 **sequential grooming. (A)** Ethograms (left) and histograms (right) showing eye grooming

781 (magenta) or wing grooming (green) elicited with red light-activated CsChrimson expressed in

782 different transgenic lines. The lines express in sensory neurons on the eyes (VT17251-LexA

783 (top row)), wings and halteres (R30B01-AD \cap R31H10-DBD (middle row)), or eyes, wings, and

784 halteres (R31H10-AD \cap R34E03-DBD (bottom row)). Data is plotted as described in **Figure 2**.

785 See **Video 6**, **Video 7**, and **Video 8** for representative examples. **(B)** GFP expression pattern of

786 R31H10-AD \cap R34E03-DBD in the CNS. Image shows a maximum intensity projection of a co-

787 stain with anti-GFP (green) and anti-Bruchpilot (magenta). Arrows indicate the body part each

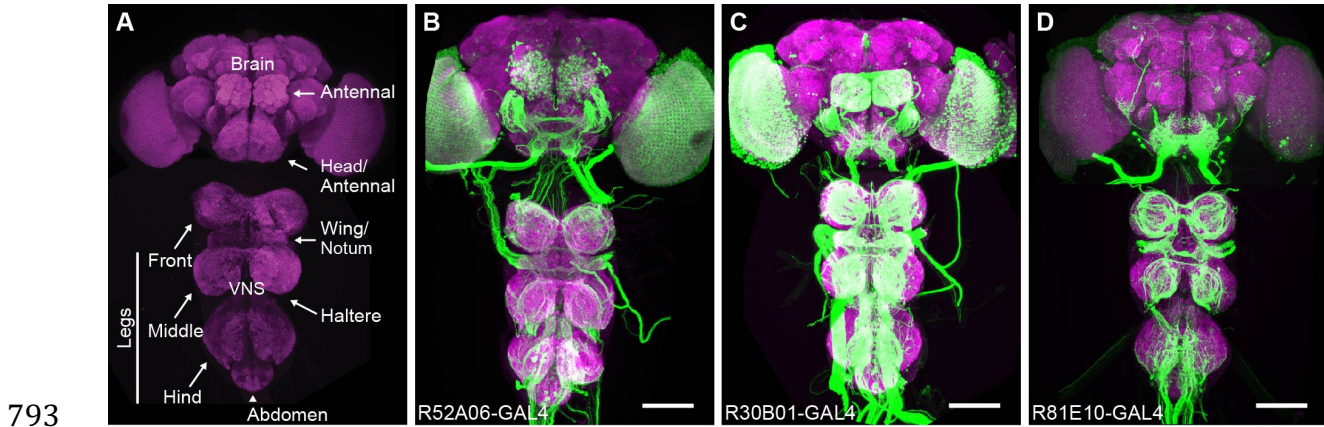
788 sensory projection is from, and the location of ascending projections from the wings and

789 halteres. Scale bars, 100 μ m.

790

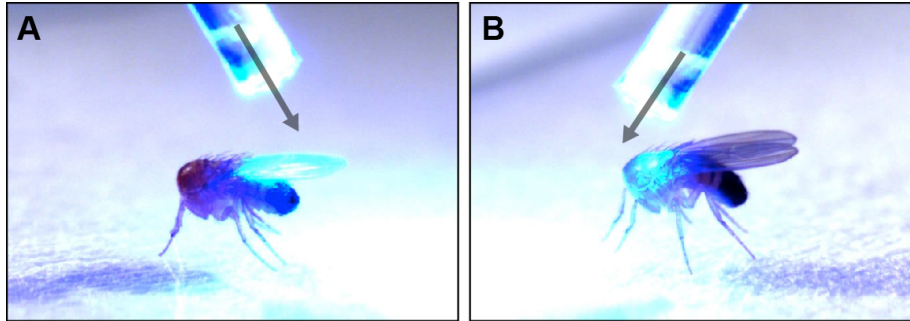
791

792



794 **Figure 1 – figure supplement 1. Anatomy of sensory GAL4 lines.** (A) Sensory neurons
795 project their axons (afferents) to specific regions of the *central nervous system* (CNS)
796 depending on which body part they are from. The neuropile of the CNS visualized with anti-
797 Bruchpilot (magenta). A confocal image maximum projection is shown. (B-D) Three different
798 GAL4 lines expressing GFP in afferent projections from the different body parts. GFP was
799 visualized with anti-GFP antibodies (green). Scale bar, 100 μ m. GAL4 lines shown are R52A06-
800 GAL4 (B), R30B01-GAL4 (C), and R81E10-GAL4 (D).

801
802
803
804
805
806
807
808



809

810 **Figure 1 – figure supplement 2. Optogenetic illumination of sensory neurons on different**

811 **body regions. (A-B)** A fiber optic probe that was connected to a blue light LED was used to

812 direct light to specific body regions. Images show illumination of the posterior (**A**) or anterior (**B**)

813 dorsal surfaces of decapitated flies. See **Video 1** and **Video 2** for representative examples.

814

815

816

817

818

819

820

821

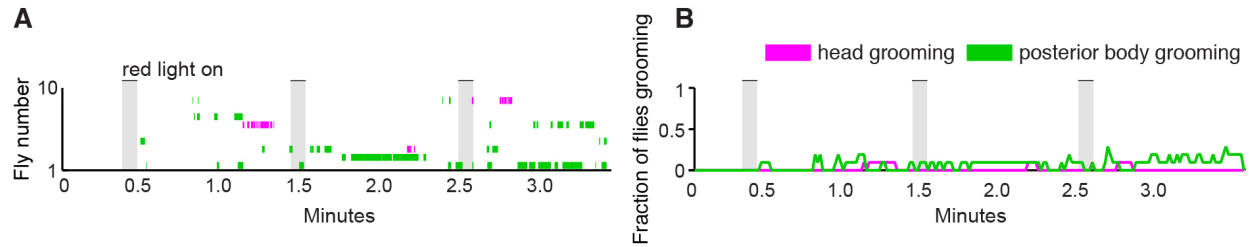
822

823

824

825

826



827

828 **Figure 2 – figure supplement 1. Illumination of control flies does not elicit grooming. (A)**

829 Ethograms showing head (magenta) or posterior body grooming (green) with red light-

830 illumination of control flies. Ethograms of individual flies are stacked on top of each other. (B)

831 Histogram shows the fraction of flies that were performing each grooming movement within one-

832 second time bins. Gray bars indicate a five second presentation of red light. This is the control

833 for the experiment shown in **Figure 2**.

834

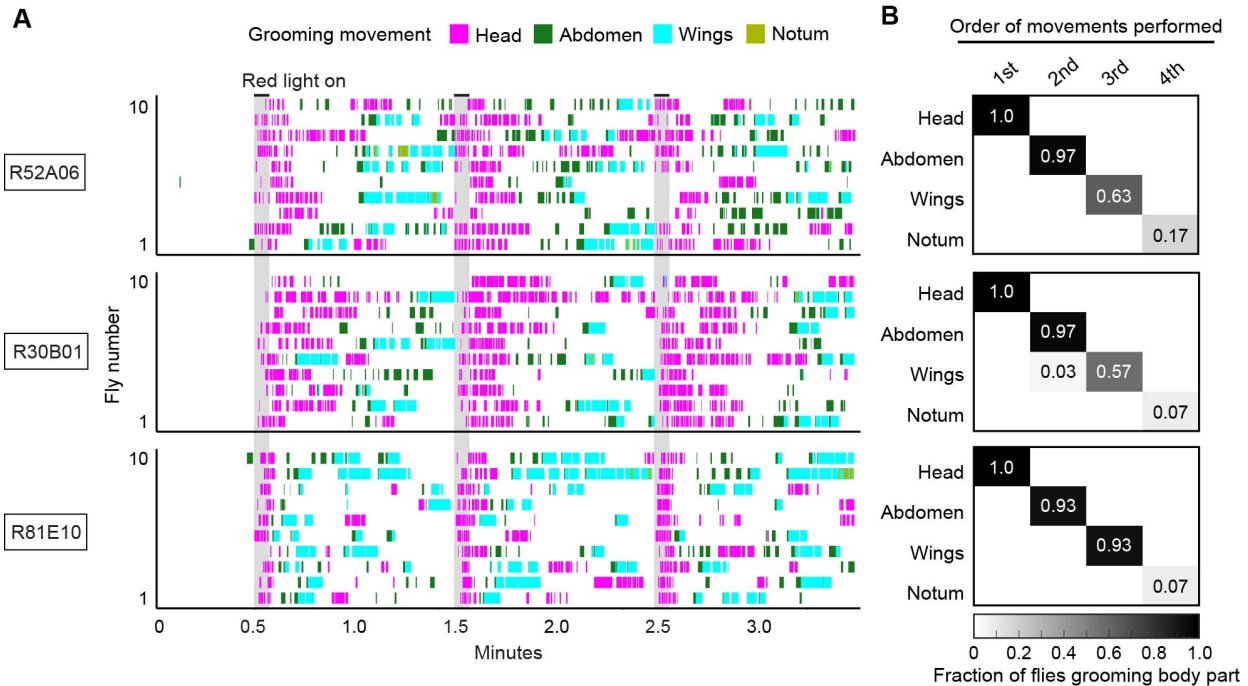
835

836

837

838

839



840

841 **Figure 2 – figure supplement 2. Simultaneous optogenetic activation of body sensory**

842 **neurons elicits a grooming sequence. (A)** Ethograms showing different grooming movements

843 elicited with red light-illumination of R52A06-, R30B01-, or R81E10-GAL4 flies expressing

844 CsChrimson. Ethograms of ten individual flies are stacked for each GAL4 line. Gray bars

845 indicate five-second presentations of a red light stimulus. Colors indicating the grooming

846 movements are shown above the ethograms. The same ethograms with binned head and

847 posterior grooming movements are shown in **Figure 2A**. **(B)** Grids show the fraction of flies

848 performing a specific grooming movement as their first, second, third, or fourth novel movement

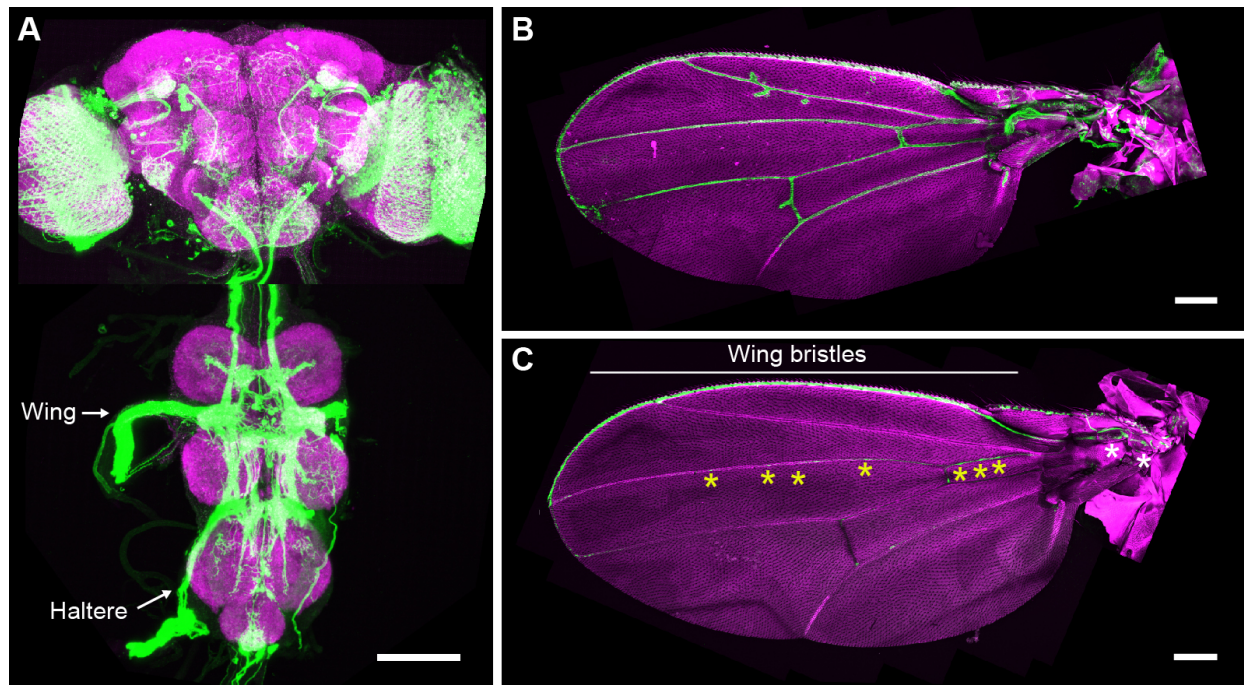
849 from the onset of the red light stimulation until the beginning of the next red light stimulus. The

850 fraction of flies performing notum grooming is low because most flies did not perform that

851 grooming movement. Notum grooming was similarly rare with dust induced grooming (Seeds et

852 al. 2014).

853



854

855 **Figure 4 – figure supplement 1. GAL4 lines that express in wing sensory neurons. CNS**
856 **(A)** and wing **(B)** expression patterns of R31H10-GAL4 that targets neurons whose activation
857 elicits wing grooming. Maximum intensity projections are shown. **(A)** The CNS expression is
858 visualized by co-staining with anti-GFP (green) and anti-Bruchpilot (magenta). Arrows indicate
859 the CNS entry points of afferents from the wings and halteres. Scale bar, 100 μm. **(B)** Wing
860 expression pattern visualized using the native GFP fluorescence in green and autofluorescence
861 from the cuticle in magenta. Scale bar, 250 μm. **(C)** Wing expression pattern of R30B01-GAL4.
862 The different symbols indicate the sensory neuron types on the wing as proximal campaniform
863 sensilla (white asterisks), distal campaniform sensilla (yellow asterisks), or bristle
864 mechanosensory (white line). Scale bar, 250 μm.